Characterization, similarity score and uniqueness associated with perspiration pattern

Aditya Abhyankar[1] and Stephanie Schuckers[1,2]

[1] Department of Electrical and Computer Engineering,
Clarkson University, Potsdam NY 13676, USA
[2] Lane Department of Computer Science and Electrical Engineering,
West Virginia University, Morgantown, West Virginia 26506, USA

Abstract. Vulnerabilities in biometric systems including spoofing has emerged as an important issue. The focus of this work is on characterization of 'perspiration pattern' in a time-series of fingerprint images for liveness detection. By using information in the high pass bands of the images the similarity score for the two images is calculated to determine the uniqueness of the perspiration pattern. In this wavelet-based approach, the perspiration pattern is characterized by its energy distribution in the decomposed wavelet sub bands. We develop a similarity matching technique that is based on quantifying marginal distribution of the wavelet coefficients. The similarity match technique is based on Kullback-Leibler distance, which is used to decide 'uniqueness' associated with the perspiration pattern. Experimental results show good separation resolution in similarity scores of inter (43 subjects) and intra (12 subjects over 5 months) class comparisons. This may be considered as a robust liveness test for biometric devices.

1 Introduction

Biometrics are gaining popularity over conventional identifiers for doing personal identification. Unfortunately, with increased technological advancement, spoofing into a fingerprint identification system has become easier. Among various fingerprint security issues, it is of particular interest to check whether source of input signal is a live genuine finger, in order to make the system intelligent enough to be able to differentiate it from a signal originating from a spoof or a cadaver. This security test added as supplement to the authentication is termed as "liveness" detection [1], [2]. It has been demonstrated that perspiration can be used as a measure of "liveness" detection in case of fingerprint matching systems [3],[4],[5],[6],[7]. Unlike cadaver or spoof fingers, live fingers demonstrate a distinctive spatial moisture pattern, when in physical contact with the capturing surface of the fingerprint scanner. This is demonstrated in Figure (1). In this paper, it is shown that this pattern, called as 'perspiration pattern', may be unique in itself across individuals. Testing of this hypothesis is performed using similarity measurements in the wavelet sub-bands. Kullback-Leibler distance on wavelet sub bands is applied and the similarity score obtained is used to demonstrate "uniqueness" associated with the perspiration pattern [8].

Fig. 1. The fingerprints captured as a time sequence. The left figure is captured at zeroth second, while the right is captured after five seconds. Perspiration is observed as time progresses in live fingers.

All natural images are by default, non-stationary, and contain several sub-images which can be exploited by varying the scale of analysis. Without extracting the exact positioning of these sub-images, direct matching of the images is not efficient. Wavelets are used to do this extraction.

In this paper, a simple sub-image decomposition using Daubechies orthogonal filters is designed. Sub-image decomposition parameters are computed to match high frequency components of the images, in order to enhance similarity score calculations. If the difference parameters are close to zero, two images are similar. Histograms of all the sub-images are calculated before performing matching.

2 Data Collection

The data required for this work was collected at Clarkson University and West Virginia University. Protocols for data collection from the subjects were followed that were approved by the Clarkson University and West Virginia University Institutional Review Board (IRB) (HS#14517 and HS#15322).

Data previously collected in our lab is used to test interclass similarity scores. This data set is diverse as far as age, sex, and ethnicity is concerned. This data set is comprised of different age groups (11 people between ages 20-30 years, 9 people between 30-40, 7 people between 40-50, and 6 people greater than 50), ethnicities (Asian-Indian, Caucasian, Middle Eastern), and approximately equal numbers of men and women. The data was collected using three different fin-

gerprint scanners, with different underlying technologies. Three scanners were chosen from three different companies namely Secugen (model FDU01), Ethentica (model Ethenticator USB 2500)and Precise Biometrics (model PS100) with optical, electro-optical and capacitive DC technique of capturing fingerprint, respectively. Following table summarizes this data.

Table 1. Data set: Distribution

Live	Capacitive DC Precise Biometric	Electro-optical Ethentica	Optical Secugen	Time span
Inter-class	31	30	30	
Intra-class	12	12	12	5 months

For analyzing intra class similarity data was collected from 12 subjects, over a period of 5 months. The subjects were asked to give their fingerprint samples at three visits and each time time-series capture was obtained three times. So, for 12 classes 9 intra class patterns were obtained.

3 Perspiration pattern extraction algorithm

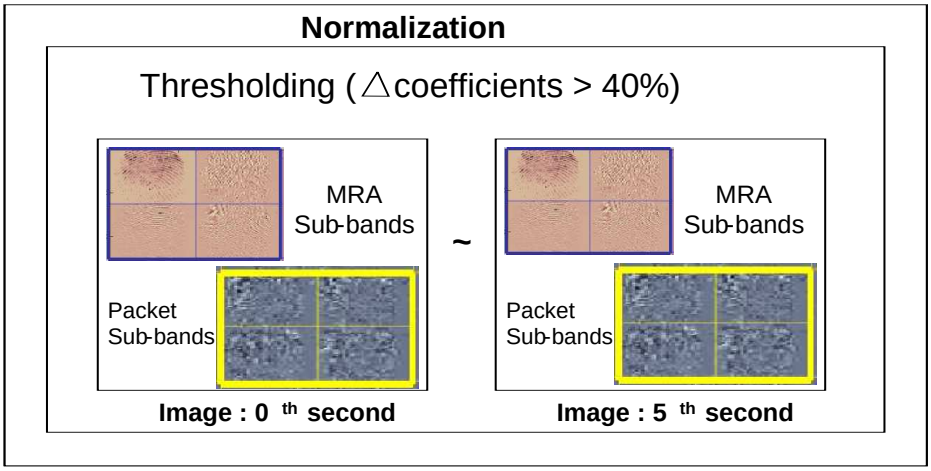

Fig. 2. Algorithm to extract perspiration pattern. Four sub-bands each form Multiresolution analysis and wavelet packets are shown separately.

The original liveness wavelet algorithm is given in detail in [5],[6],[7]. The algorithm uses Daubechies wavelet-based approach to decompose 0 second image and second image at either 2 or 5 seconds. Maxima energy extraction is done after initial image enhancement for both the images. Multiresolution analysis is used to process LP information, while wavelet packets are used to extract information form HP bands. Only those coefficients are retained which experience more than 40% change in the energy content from the first to last image. Normalization is done by the energy content of the later image to account for pressure variations. The entire algorithm in snap shot is given in Figure (2).

Total energy associated with the changing coefficients, normalized by total energy of the second image is used as a measure to decide the "liveness" associated with the scanner. It is given by following formula,

Formula: "liveness measure"

$$e\% = \left(\frac{\sum \text{energy of sub bands of the thresholded difference image}}{\sum \text{energy of sub bands of the image captured after five seconds}}\right) \times 100 \tag{1}$$

The retained coefficients relate directly to the perspiration pattern as shown in the reconstructed images in Figure (3). The following section describes the sub-level decomposition using wavelets. These coefficients will be used in assessing the uniqueness of perspiration patterns. The scales selected for the algorithm are 2 and 3 for mulriresolution analysis and wavelet packet analysis, respectively. The basis is formed by ψ as well as ϕ.

4 Sub-level decomposition of images and pattern characterization

Assuming existence of nested sequences of subspaces $\{V_j\}_{j=-\infty}^{\infty}$ the selected set of Daubechies scaling functions is $\{\phi(x-k)\}_{k\in Z}$ is an orthonormal basis,i.e.,

$$\int_{-\infty}^{\infty} \phi(x-k)\phi(x-k')dx = \begin{cases} 0,\ k \neq k',\ \ k,k' \in Z \\ 1,\ k = k' \end{cases} \tag{2}$$

For the vector space V_j spanned by the discrete scaling functions $\{\phi(2^j x-k)\}$, $f_j(x) \in V_j$ [9],

$$f_j(x) = \sum_k \alpha_{j,k} 2^{\frac{j}{2}} \phi(2^j x - k) \tag{3}$$

$$\alpha_{j,k} = \int_{-\infty}^{\infty} f(x) 2^{\frac{j}{2}} \phi(2^j x - k)dx \tag{4}$$

and the set $\{\phi(2^j x - k)\}$ constitutes the basis.

Now $V_j \in V_{j+1}$, and V_{j+1} has better refinement than V_j. This "difference" is a subset of V_{j+1} spanned by the discrete wavelets of the subspace W_j, $g_j(x) \in W_j$,

$$g_j(x) = \sum_k \beta_{j,k} 2^{\frac{j}{2}} \psi(2^j x - k) \tag{5}$$

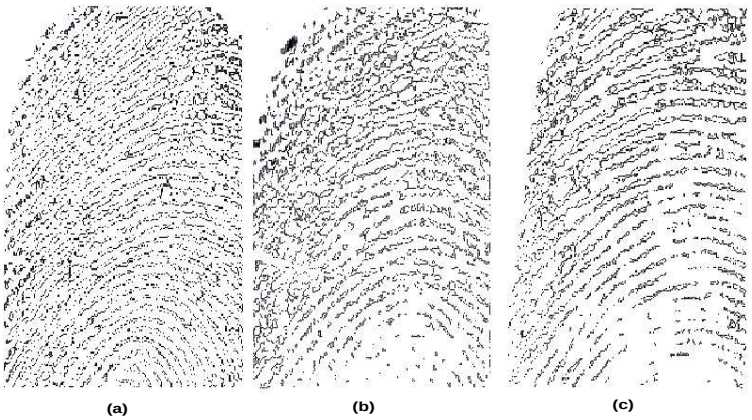

Fig. 3. (a)-(b)-(c) show perspiration patterns for three different subjects. Although these patterns are directly related to the energy changes, they are not normalized and hence are not exactly the same energy measures as given in formula (1).

$$\beta_{j,k} = \int_{-\infty}^{\infty} f(x) 2^{\frac{j}{2}} \psi(2^j x - k) \tag{6}$$

The basis $\{\psi(2^j x - k)\}$ of this vector space W_j are always orthogonal to the scaling functions $\{\phi(2^j x - k)\}$ of V_j on $(-\infty, \infty)$,

$$\int_{-\infty}^{\infty} 2^{\frac{j}{2}} \phi(2^j x - k) 2^{\frac{j}{2}} \psi(2^j x - k') dx = \delta_{k,k'} \tag{7}$$

4.1 Orthogonal wavelet filters

The wavelet filters $LP_{k,l}$,$\widetilde{LP_{k,l}}$,$HP_{m,l}$ and $\widetilde{HP_{m,l}}$ form an orthogonal filter set if they satisfy following conditions,

$$< LP_{k,l}, \widetilde{LP_{k',l}} >= \delta_{k,k'} \tag{8}$$

$$< HP_{m,l}, \widetilde{HP_{m',l}} >= \delta_{m,m'} \tag{9}$$

$$< LP_{k,l}, HP_{m,l} >= 0 \tag{10}$$

where, $LP_{k,l}$ and $HP_{m,l}$ stand for low pass and high pass decomposition filters, while $\widetilde{LP_{k,l}}$ and $\widetilde{HP_{m,l}}$ are reconstruction filters. Low pass filters come form ϕ functions, while high pass filters come form ψ functions.

If the base image is denoted by $IM^1_{i,j}$, then applying both low as well as high filters in horizontal and vertical directions would result in four sub-bands,

namely LL, HL, LH and HH. They can be written as,

$$LL^0_{k,k'} = \sum_{i,j} \widetilde{LP_{k,i}} \widetilde{LP_{k',j}} IM^1_{i,j} \tag{11}$$

$$LH^0_{k,m} = \sum_{i,j} \widetilde{LP_{k,i}} \widetilde{HP_{m,j}} IM^1_{i,j} \tag{12}$$

$$HL^0_{m,k} = \sum_{i,j} \widetilde{HP_{m,i}} \widetilde{LP_{k,j}} IM^1_{i,j} \tag{13}$$

$$HH^0_{m,m'} = \sum_{i,j} \widetilde{HP_{m,i}} \widetilde{HP_{m',j}} IM^1_{i,j} \tag{14}$$

Here, $LL^0_{k,k'}$ is the low frequency component, $LH^0_{k,m}, HL^0_{m,k}, HH^0_{m,m'}$ are the high frequency components in horizontal, vertical and diagonal directions, respectively, after decomposing the image. Since, the filters used are orthogonal filters, as they follow properties in equation (2), the original image can be reconstructed from these sub-bands using following reconstruction formulae [10],

$$\begin{aligned} IM^1_{i,j} = \ & \textstyle\sum_{k,k'} \widetilde{LP_{k,i}} \widetilde{LP_{k',j}} IM^1_{i,j} + \sum_{i,j} \widetilde{LP_{k,i}} \widetilde{HP_{m,j}} IM^1_{i,j} + \\ & \textstyle\sum_{m,k} \widetilde{HP_{m,i}} \widetilde{LP_{k,j}} IM^1_{i,j} + \sum_{m,m'} \widetilde{HP_{m,i}} \widetilde{HP_{m',j}} IM^1_{i,j} \end{aligned}$$

This formula, after extending it to the respective levels of decomposition for MRA and packet analysis, can be used to visualize the perspiration pattern, after doing the thresholding. By the end of the process we will have 1 LL band and 7 high pass bands, coming from MRA and packet analysis. Sub-band alignment is performed as the complete algorithm itself is sub-band oriented. The MRA uses LL band and computes $IM^{-1}_{i,j}$, while packet analysis gives $IM^{-2}_{i,j}$, where the basis is adaptive and is calculated using Shannon entropy [7]. Thus, for MRA we get our output from $V_{-2} \oplus W_{-2} \oplus W_{-1}$ and for packet analysis we get our output from $V_{-3} \oplus W_{-3} \oplus W_{-2} \oplus W_{-1}$. Essentially, after thresholding, the method measures energy at the output of filter banks as extracted perspiration pattern. The main idea behind the algorithm is that energy distribution in energy domain identifies a pattern [7].

5 Similarity Measurement

The energy distribution described above is the pattern being considered to analyze similarity between inter and intra class perspiration patterns, score based on the 'Kullback-Leibler' distance between two images is calculated [8]. The Kullback-Leibler distance is essentially a relative entropy between two densities d_1 and d_2, and is given as [11],

$$D(d_1||d_2) = \int f \log \frac{d_1}{d_2} \tag{15}$$

where, densities d_1 and d_2 represents two images under consideration. This is an attempt to characterize the perspiration pattern via marginal distributions of their wavelet sub-band coefficients [12].

Generalized Gaussian density (GGD) is defined as,

$$p(x;\alpha,\beta) = \frac{\beta}{2\alpha\Gamma(1/\beta)} e^{-(\frac{|x|}{\alpha})^{\beta}} \tag{16}$$

where, $\Gamma(.)$ is the Gamma function, so,

$$\Gamma(z) = \int_0^{\infty} e^{-t} t^{z-1} dt, z > 0$$

Here, α is variance and β is inversely proportional to the decreasing peak frequency. A good probability density function (PDF) approximation for the marginal density of coefficients at a particular sub-band (2 for MRA and 3 for packets for this algorithm), is achieved by adaptively varying α and β of GGD. Marginal distributions give better representation of of perspiration pattern than the wavelet sub-band energies.

Using equations (15) and (16), closed form of the KLD is given as [12],

$$D(p(.;\alpha_1,\beta_1)||p(.;\alpha_2,\beta_2)) = \log(\frac{\beta_1\alpha_2\Gamma(1/\beta_2)}{\beta_2\alpha_1\Gamma(1/\beta_1)}) + (\frac{\alpha_1}{\alpha_2})\frac{\Gamma((\beta_2+1)/\beta_1)}{\Gamma(1/\beta_1)} - \frac{1}{\beta_1} \tag{17}$$

The similarity measurement between two wavelet sub-bands can be computed very efficiently using the model parameters.

The overall distance between the images can be given as follows,

$$D(IM_1, IM_2) = \sum_j D(p(.;\alpha_1^j,\beta_1^j)||p(.;\alpha_2^j,\beta_2^j)) \tag{18}$$

This is because of the scalable nature of the wavelet transform. The wavelet coefficient in different sub-bands are independent, and so to find the overall score, individual KLDs are summed up. Here, j is the sub-band level [13],[12].

6 Experimental Results

The experimental calculations are done on the data set mentioned in section (2). Statistical independence of the perspiration patterns is directly proportional to the degrees of freedom used for doing similarity analysis. Moreover more degrees of freedom results in a more complex system. We continued to use 10000 maximum energy extracted points by the algorithm in [5]. 820 interclass and 72 intra-class combinations were exploited. As, for the intra-class scores, as the data collection was performed over 5 months, consistency factor of the perspiration pattern is also studied. No environmental conditions are tested intentionally.

The wavelet coefficients obtained from the algorithm [5], were used for further processing. The similarity score between the images is calculated using equation (17). This form of KLD is easy to implement and is found better than other close

techniques like Bhattacharya coefficient [11]. A smaller similarity score indicates a better match. The in-band matching is done for individual bands, and then the scores are added and normalized. No further thresholding is implemented as the coefficients are already thresholded.

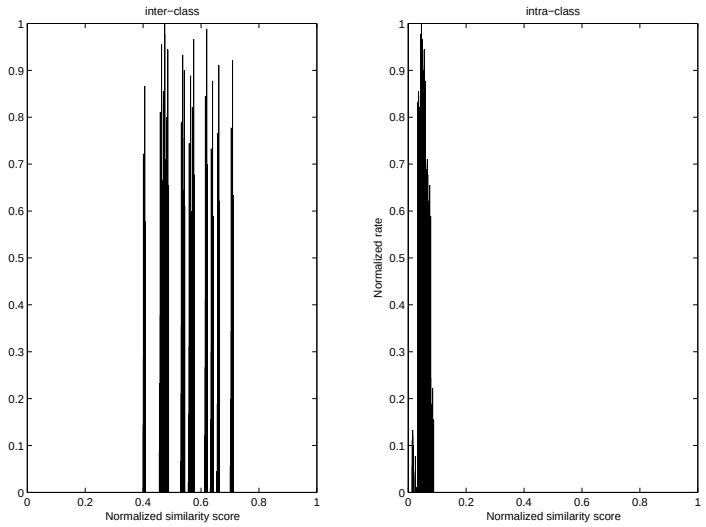

Fig. 4. Results of characterization of perspiration pattern. Similarity scores for inter and intra-class patterns. The similarity score is normalized. The intra class can be seen very similar, and inter class can be seen distributed around 0.6, and hence very much random.

Results are shown in Figure (4). The normalized rates are plotted on the y-axis and normalized similarity scores are plotted on x-axis. Inter class distribution is observed to be random, while intra class distribution is observed to be similar. Hardly any variation in the intra-class distribution is observed, thus confirming the consistency in the perspiration pattern of the 12 subjects over the period of 5 months. Distinct separation between the two classes is seen.

7 Conclusion

The perspiration pattern was observed to be 'unique' for the limited data set. The pattern also showed good consistency within the same class when monitored over 5 months. It is required to explore this matter with much wider data set, for

different environmental conditions and to see the exact relation between sweat pores and this pattern. Previous work in liveness using perspiration pattern used general features across all the subjects to specify liveness. By expecting a specific liveness pattern from an individual, the liveness algorithm may be more robust to attacks. Beyond its possibility as a biometric alone or more promisingly in conjunction with fingerprint, the method of unique liveness detection in fingerprint scanners can decrease the vulnerability of biometric devices to spoof attacks.

Acknowledgements:
We would like to acknowledge funding from National Science Foundation (0325333) with co-funding from the Department of Homeland Security.

References

1. Davide Maltonie, Dario Maio, Anil K. Jain, and Salil Prabhakar. *Handbook of Fingerprint Recognition.* Springer-Verlag New York, Inc., 2003.
2. N. Ratha. Enhancing security and privacy in biometrics-based authentication systems. *IBM systems journal*, 40:614–6134, 2001.
3. Reza Derakshani, Stephanie Schuckers, Larry Hornak, and Lawrence Gorman. Determination of vitality from a non-invasive biomedical measurement for use in fingerprint scanners. *Pattern Recognition Journal*, 36(2), 2003.
4. Stephanie Schuckers. Spoofing and anti-spoofing measures. In *Information Security Technical Report*, volume 7, pages 56–62, 2002.
5. Aditya Abhyankar and Stephanie Schuckers. Wavelet-based approach to detecting liveness in fingerprint scanners. *Proceedings of the SPIE Defense and Security Symposium, Biometric Technology for Human Identification*, April 2004.
6. Stephanie Schuckers and Aditya Abhyankar. Detecting liveness in fingerprint scanners using wavelets: Results of the test dataset. *Proceedings of the Biometric Authentication Workshop, ECCV,*, May 2004.
7. Aditya Abhyankar. *A Wavelet-based approach to detecting liveness in fingerprint scanners.* Master's thesis, 2003.
8. S. Kullback and R. A. Leibler. On information and sufficiency. *Ann. Math. Stat*, 22:7986 1951.
9. Ingrid Daubechies. *Ten Lectures on Wavelets.* Society of Industrial and Applied Mathematics, 1998.
10. Ingrid Daubechies, Yves Meyer, Pierre Gilles Lemerie-Rieusset, Philippe Techamitchian, Gregory Beylkin, Ronald Coifman, M. Victor Wickerhauser, and David Donoho. Wavelet transform and orthonormal wavelet bases. In *Different Perspectives on Wavelets*, volume 47, pages 1–33, San Antonio, Texas, Jan. 1993.
11. Don H. Johnson and Sinan Sinanovi. Symmetrizing the kullback-leibler distance. *IEEE Trans. Image Proc*, March 2001.
12. M. N. Do and M. Vetterli. Wavelet-based texture retrieval using generalized gaussian density and kullback-leibler distance. *IEEE Trans. Image Proc*, Dec 1999.
13. T. Chang and C.-C. J. Kuo. Texture analysis and classification with tree-structure wavelet transform. *IEEE Trans. Image Proc*, 2(4) 1993.